Materials Research. 2019; 22(1): e20170804
DOI: http://dx.doi.org/10.1590/1980-5373-MR-2017-0804

Effect of Aging Heat Treatment H950 and H1000 on Mechanical and Pitting Corrosion Properties of UNS S46500 Stainless Steel

Camila Haga Beraldo[a], José Wilmar Calderón-Hernández[a]*, Rodrigo Magnabosco[b], Neusa Alonso-Falleiros[a]

[a]*Departamento de Engenharia Metalúrgica e de Materiais, Escola Politécnica, Universidade de São Paulo, São Paulo, SP, Brasil*
[b]*Departamento de Engenharia de Materiais, Centro Universitário FEI, São Bernardo do Campo, SP, Brasil*

Received: September 05, 2017; Revised: May 30, 2018; Accepted: October 11, 2018

The effect of aging temperature on mechanical and pitting corrosion properties of UNS S46500 was investigated. Tensile and Hardness tests were carried out and the microstructure was analyzed by optical microscopy, scanning electron microscopy and X-ray diffraction; Thermo-Calc simulations helped in the phase identification. Pitting corrosion properties were investigated in 0.6M NaCl electrolyte with sulfate additions by Potentiodynamic Polarization (PP). Hardness, tensile and yield strength of the UNS S46500 steel after lower aging temperature, 510ºC (H950), are higher than the ones found in the 538ºC (H1000) aged steel.This result is explained by microstructure, X-ray diffraction and Thermo-Calc analysis, which indicated the presence of austenite, chi phase and probably Ni_3Ti precipitates finely and uniform distributed throughout the martensite matrix. Pitting corrosion resistance is equivalent in both aging temperatures. The sulfate inhibitor effect on UNS S46500 steel was enhanced for 538ºC condition when the electrolyte reaches $1Cl^-$:$1SO_4^{2-}$ ratio, which is explained by Ni sulfate adsorption and the amount of interfaces in the microstructure resulting in smaller amount of adsorption sites, such as coarsened Ni_3Ti precipitates, smaller fraction of chi phase and recovery of dislocations in martensite structure.

Keywords: *martensitic precipitation hardening stainless steel, aging heat treatment, pitting corrosion.*

1. Introduction

The mechanical properties of precipitation hardening steels can be attributed to the presence of a fine and uniformly distributed intermetallic particles in a martensitic matrix[1]. The UNS S46500 steel is strengthened by precipitation of Ni_3Ti. It is known [2] that longer aging times and/or higher aging temperatures imply in growth and coarsening this precipitates, leading to mechanical properties reduction.

The heat treatment of these materials is accomplished by solution heat treatment followed by water or oil quenching. The presence of retained austenite is possible and a quick cryogenic treatment is employed to further reduce or eliminate the fraction of retained austenite. However, when high toughness and high strength material is desired, the presence of low quantities of this phase is important. Schnitzer et al.[3] proposed that austenite is formed during the aging of the material, and this austenite is called reverted austenite, which is formed at the same time of precipitates nucleation in the martensitic matrix, i.e. the austenite stabilizer element, Ni, is present in the precipitate nucleation Ni-X and simultaneously there is its diffusion into less ordered regions, e. g. grain boundaries or martensite lath boundaries, occurring its microsegregation and leading to austenite nucleation.

The precipitation hardening stainless steels have been widely used in aerospace application due to its combination of strength, toughness and corrosion resistance[4-5]. In this material, the main form of corrosion is the localized corrosion (pit and crevice), where cavities formed act as stress concentrator, which can lead the material to a catastrophic failure[5].

Pitting corrosion can be studied by many methods, such as potentiodynamic polarization, salt spray, weight loss, always in the presence of chloride ion. In the potentiodynamic polarization test, the pitting potential (Epit) is measured relative to a reference electrode in different environments depending on the purpose of the study. Some electrolytes, when excessively aggressive, do not permit the Epit determination, since they promote general surface corrosion, or present a lack of sensitivity to distinguish the difference between pitting corrosion resistance where its properties are similar. The addition of inhibitors compounds in these electrolytes can improve the sensitivity and allow differentiation in the materials performance [6-7]. In this investigation was used 0.6M NaCl electrolyte with sulfate additions to decrease the aggressively and try to differentiate the performance of the steels.

*e-mail: wilmarcalderon100@gmail.com.

Thus, the combination between mechanical and corrosion properties shall be evaluated when these materials are applied. UNS S46500 has as peak strength aging temperature 482ºC (900ºF) [2]. However, this temperature will provide the highest strength but not necessarily the best corrosion resistance. In fact, this aging cycle promotes the sensitivity to stress corrosion cracking. Thus, there are limitations on aging temperatures used for precipitation hardening stainless steels. For the UNS S46500, the suggested aging temperature for optimum strength and corrosion resistance is known as H950 and H1000 according to AMS 5963[8]. Both are carried out for 4 hours, varying only the aging temperature, where for H950 is 510ºC (950ºF) and for H1000 is 538ºC (1000ºF).

The purpose of this study is to clarify the effect of aging condition, H950 or H1000, on the mechanical properties and localized corrosion resistance of martensitic precipitation hardening stainless steel UNS S46500.

2. Experimental Procedures

The chemical composition of investigated martensitic precipitation hardening stainless steel is given in Table 1. This material, trade named as Custom 465®, was provided by Carpenter Technology Inc. in the form of a solution heat treated rolled bar with 25.4 mm of diameter, and was then subjected to different aging treatments, 510ºC (H950) and 538ºC (H1000), both for 4 hours according to AMS 5963[8]. The tests and microstructure examination was done for UNS S46500 on solution heat treated, H950 or H1000 conditions.

Tensile tests were conducted on Wolpert type 20TUZ 750 equipment. For each aging condition, 6 cylindrical specimens with a diameter of 6 mm were tested in the longitudinal direction and tensile elongation values were measured on a 25 mm Panantec gage length according to ASTM E8/E8M[9]. The tensile test at ambient temperature was registered by Panantec ATMI software. Three measurements of Rockwell C (HRC) hardness test, conducted on Pantec RBS, was performed directly on transversal direction of heat treated bars according to ASTM A370[10].

The specimens were metallographically polished up to 1 µm and then examined with and without Vilella (1 g picric acid, 5 mL hydrochloric acid, 100 mL ethanol)[11] and Fry (5 g copper(II) chloride, 33 mL hydrochloric acid, 33 mL ethanol, 33 mL distilled water)[11] etching, at room temperature and with immersion times between 15 and 30s.

Metallographic specimens were observed in an optical microscopy (OM). It was also used a scanning electron microscopy (SEM), Jeol JSM-6490LV, generating secondary electron images and energy-dispersive X-ray analysis.

X-ray diffraction patterns were obtained using Cu-Kα radiation (wavelength of 1.5418 nm), at 30 kV and current of 30mA at Shimadzu XRD-7000 diffraction equipment. Scan rate of 2º/min e scan step of de 0.04º were used.

Potentiodynamic polarization tests were conducted in a plane cell (leaving a working area of 1 cm^2) using potentiostat/galvanostat 273A Princeton Applied Research and 352 SoftCorr III software. The working surface of disks with 24 mm diameter and 6 mm height was ground subsequently up to 600 grit SiC paper, cleaned with distilled water and alcohol, and dried in cold air. The test solution was 0.6M NaCl electrolyte with Na_2SO_4 additions (0.06M; 0.3M; 0.6M) to decrease the aggressiveness of the electrolytes, allowing a better differentiation of the heat treatment conditions' performance, The steel specimen was used as working electrode, platinum wire with 1 mm diameter and 25 mm long as counter electrode and a silver/silver chloride (Ag/AgCl) electrode as reference electrode. The specimen was cathodically polarized at 250 mV, followed by potential scan, with scan rate of 1 $mV.s^{-1}$, up to current density of 10^{-3} $A.cm^{-2}$. Pitting potential (Epit) was read directly on polarization curve at the potential which the anodic current increased abruptly. The electrochemical tests, performed at room temperature (23 + 2 ºC), were repeated 10 times for each heat treatment condition. Immediately after the polarization, sample surfaces were washed with distilled water and then with ethyl alcohol (C_2H_5OH), and finally dried with hot blown air and observed in optical and scanning electron microscopy in order to analyze the corroded surface morphology.

3. Results

Table 2 shows the average results of mechanical properties. For both aging conditions, H950 and H1000, the tensile strength, yield strength, elongation (EL) and hardness values are above the typical specifications of AMS 5963[8], which are 47 HRC of hardness, yield strength of 1515 MPa, tensile strength of 1655 MPa and total elongation of 10%. It is possible to observe that increasing the aging temperature leads to the reduction of the tensile and yield strengths, and a slight tendency to decrease of hardness, while elongation increased. This result is in accordance with previous works[4,12-13], for instance the results found by Xiang et al.[12]and Narendra

Table 2. Mechanical properties of the aged conditions studied.

Heat Treatment	Tensile Strength (MPa)	Yield Strength (MPa)	EL (%)	Hardness (HRC)
H950	1881 ± 21	1836 ± 22	10 ± 0.5	52 ± 1
H1000	1702 ± 14	1676 ± 15	12 ± 0.9	49 ± 3

Table 1. Chemical composition (wt.%) of the investigated UNS S46500.

C	Mn	Si	P	S	Cr	Ni	Mo	Ti	N	Fe
0.005	0.02	0.04	0.003	0.0005	11.63	11.02	0.94	1.59	0.002	Balance

et al.[13], the first authors aged the steels at 550ºC, 580ºC and 620ºC reporting maximum hardness at 550ºC (33.1 HRC) and minimum at 620ºC (28 HRC). On the other hand, Narendra et al.[13] carry out aging heat treatments from 510ºC (H950) to 570ºC with intervals of 20ºC and several time conditions, it was report that specimen aging heat treated at 510ºC during 2h had maximum hardness but the values were not informed in that paper. A recent review paper reports hardness value of 49 HRC for the H950 condition[4].

The microstructure analysis of polished specimens, solution heat treated, H950 and H1000 revealed the presence of disperse titanium nitride particles in the metallic matrix. Figure 1 and Table 3 show the morphology of titanium nitride (TiN) particles and the EDS results of particle and matrix of steel on H950 aging condition confirming that the particle is enriched with titanium.

Figure 2 shows the optical micrographs of Vilella etched specimens. As observed in the Lee et al.[14] work, the main microstructural feature consists of martensite lath packets with different orientation within relatively equiaxed prior austenite grains. The titanium nitride precipitates observed in the polish specimens where also observed after etching.

Investigations by SEM (Figures 3-5) show more clearly the microstructural differences of three heat treated conditions (solution heat treated, H950 and H1000). The evaluation of the same heat treated condition, it is possible to observe that the different metallographic etched of solution specimens did not revealed differences in the quantity and distribution of precipitates and phases. However, for the aging specimens, H950 and H1000, the Vilella etch revealed more pronounced the martensite lath, white phases and grain boundaries.

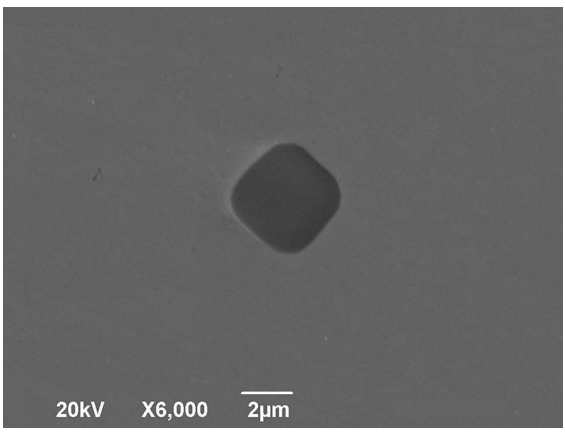

Figure 1. SEM image of polished (up to 1µm) H950 specimen showing the titanium nitride. EDS analysis on precipitate and matrix is shown at Table 3.

The comparison between the three heat treated conditions (solution heat treated, H950 and H1000) revealed increased quantity of white phase (Figures 3 to 5) for aged conditions than solution heat treated specimens; and the Figure 6 show that H950 present higher fraction of white phases than for H1000 condition. The EDS of solution heat treated specimen revealed that the white phase is enriched by Mo and Ti elements (Figure 7 and Table 4). It was not possible see the white phase using the backscattered electrons detector (by chemical composition), only with the secondary electrons detector which gives information about the morphology of matrix. Complementing the microscopy analysis, Figure 8 shows the X-ray diffraction patterns of three heat treatment condition, solution heat treated, H950 and H1000. According the XRD analysis all heat treatment conditions indicate the presence of body-centered cubic phase which represents the martensite (α) matrix . Equilibrium phase simulation for the aged conditions (Table 5) predicted the formation of chi (χ) phase in both aging conditions, but the small fractions of expected equilibrium chi phase, and its diminute dimensions resulted from the precipitation process, did not allowed its identification by XRD. In the same way, TiN observed in the OM and SEM images were not found in the X-ray diffractions, and this can be atributted to lower fraction of nitrogen (0.002%) on the steel chemical composition, leading to very small volume fractions of TiN, not detectable by X-ray diffration.

Thermodynamic simulations in Thermo-Calc software using TCFE8 database was performed; whereas the aging treatments H950 and H1000 occurring at 510ºC and 538ºC respectively, the equilibrium phases and its volume fractions at those temperatures are presented in Table 5, and some considerations about this simulation can be addressed:

BCC phase, body centered cubic ferrite, is the martensite matrix structure.

Ni_3Ti precipitates are responsible for strength the material. They were not observed on OM, SEM and X-ray diffraction analysis, since their very small size, however the literature[2,15] indicates their presence. The tensile mechanical properties of the UNS S46500 can be attributed to a precipitation of a fine and disperse distribution of these precipitates in the martensite matrix. The identification of Ni_3Ti is possible with specialized research and major microscopy resolution as transmission electron microscopy (TEM).

Chi phase, according to studies[16], is enriched with Fe, Cr and Mo ($Fe_{36}Cr_{12}Mo_{10}$)[16], and was observed in the microscopy analysis for both aging conditions.

Table 3. Chemical composition of matrix and precipitate of Figure 1.

Elements (wt.%)	Cr	Ni	Ti	N	Fe
Matrix	11.74	12.32	1.81	-	74.13
Precipitates	-	-	81.93	13.79	4.29

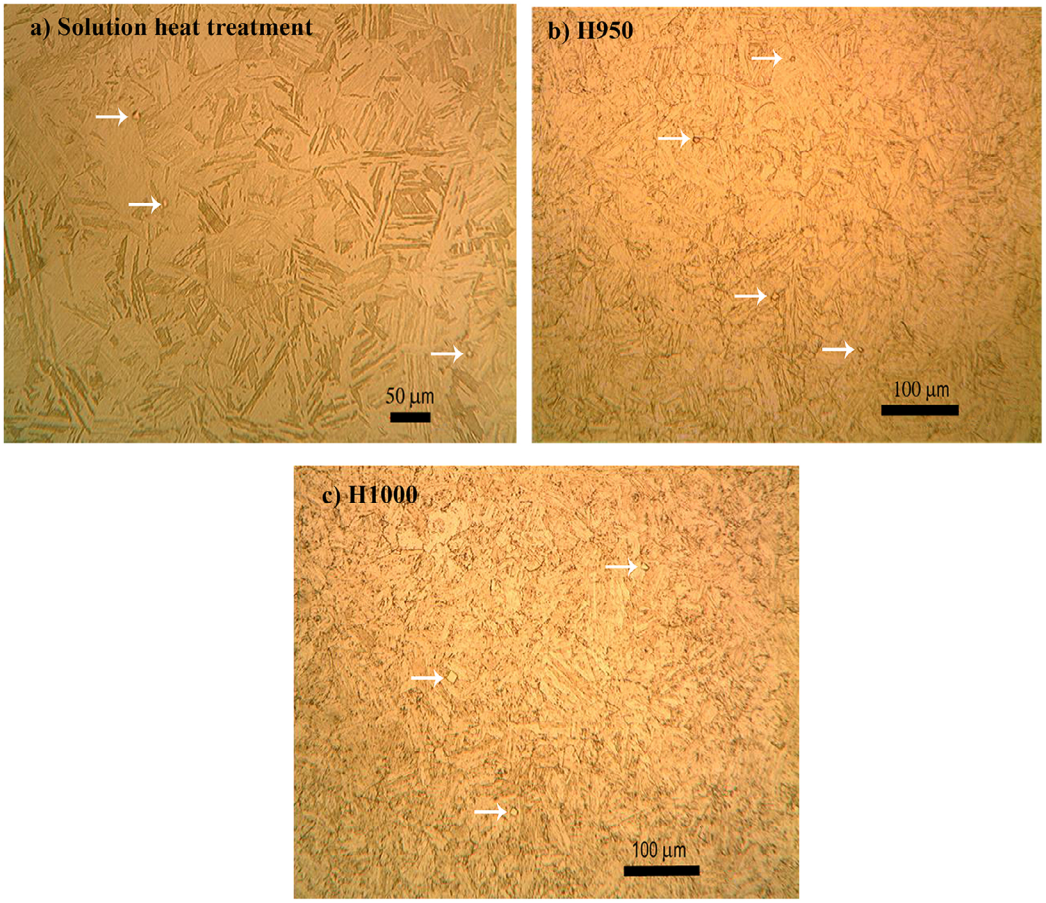

Figure 2. OM images of specimens: (a) solution heat treatment; (b) H950 and (c) H1000; Vilella etched. Martensite with few titanium nitride particles indicated by arrows.

FCC phase, face centered cubic austenite, were not observed on OM and SEM analysis, however it is mentioned in the literature works[3].

The quantity analysis of Thermo-Calc indicated that the main difference between H950 and H1000 aging condition is in the quantity of austenite and chi phase, as observed in the Table 5.

Thus, the Thermo-Calc analysis and OM, SEM, EDS and X-ray diffraction tests results indicate that the UNS S46500 steel in the H950 and H1000 aging present a martensite matrix with Ni_3Ti and chi precipitates, and some austenite phase.

Figure 9 show typical polarization curves of UNS S46500 in each heat treatment condition. The polarization tests results of solution heat treated material was used as corrosion reference for the material in the aging conditions.

The polarization curves show a cathodic region followed by passive region under all heat treated conditions, and the Epit appear defined in all polarization curves. It is also observed that when the sulfate addition achieves 1:1 of Cl^-:SO_4^{-2}, the Epit marked increased compared with other electrolytes concentrations.

The average and deviation of Epit obtained on polarization curves are indicated at Figure 10. The analysis of Epit for both aging conditions indicated that the Epit increased with SO_4^{-2} addition, which indicates that the pitting corrosion resistance increased. This behavior is expected since the literature[17-18,19]indicates the inhibitor effect of this ion for stainless steels. It is also observed that the inhibitor effect of SO_4^{-2} for UNS S46500 steel in H1000 condition is enhanced gradually with increased SO_4^{-2} additions, allowing it to reach the highest Epit for this condition when the electrolyte is in proportion to 1Cl^-: 1 SO_4^{-2}.

Analyzing the polarization curves in terms of current density (Figure 9), it is clear that the material in both conditions are in the passive state, showing current densities between 10^{-5} and 10^{-6} A/cm^2, nevertheless the evaluated conditions using only 0.6M NaCl always showed slightly higher current density before reach the Ep indicating that this chloride concentration affects the passive layer more pronouncedly.

It is known that pitting corrosion can be evaluated by mean of several parameters, among these are, Ep, pit depth, pits density and pit mouth morphology. In this work, it was used the parameters of Ep and pit mouth morphology

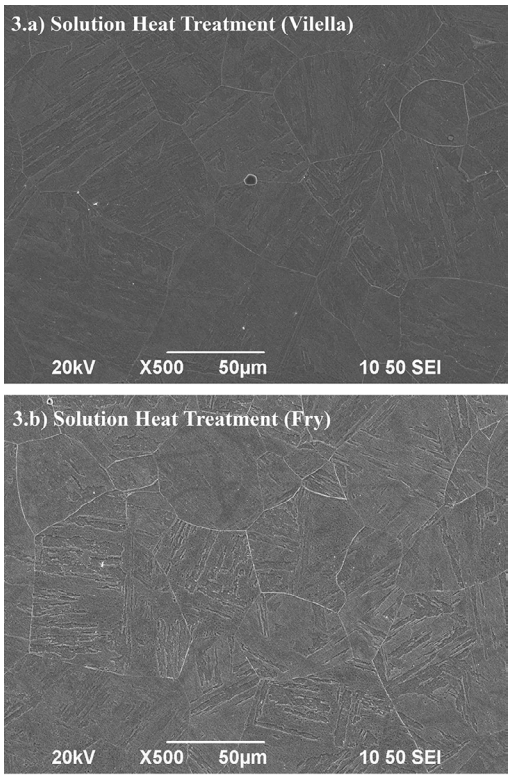

Figure 3. SEM images of solution heat treated condition, etched with: (a) Vilella and (b) Fry.

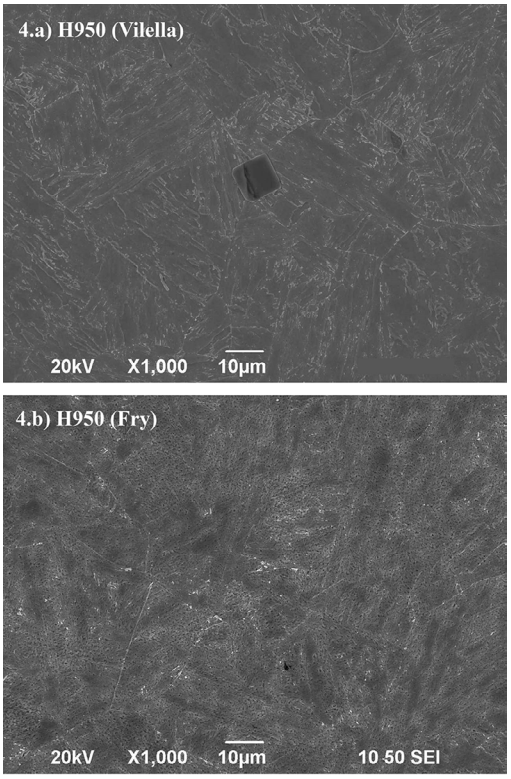

Figure 4. SEM images of H950, etched with: (a) Vilella and (b) Fry.

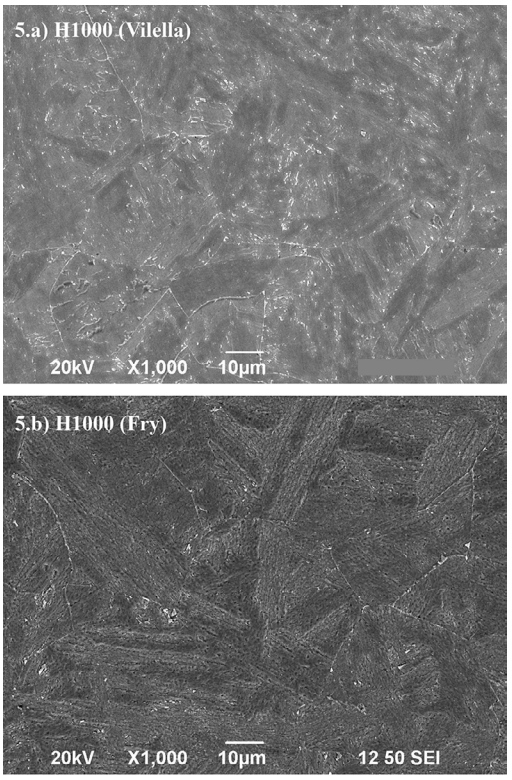

Figure 5. SEM images of H1000, etched with: (a) Vilella and (b) Fry.

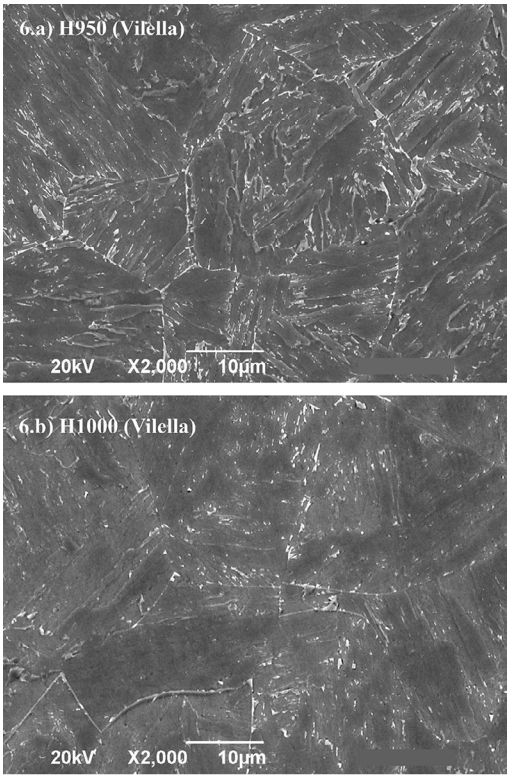

Figure 6. SEM images of (a) H950 and (b) H1000, etched with Vilella, showing the quantity difference of white precipitates.

(Figure 11) to infer that different heat treatments did not alter the pitting mechanism, explaining the equivalent pitting potential for the different heat treatment conditions in the same electrolyte.

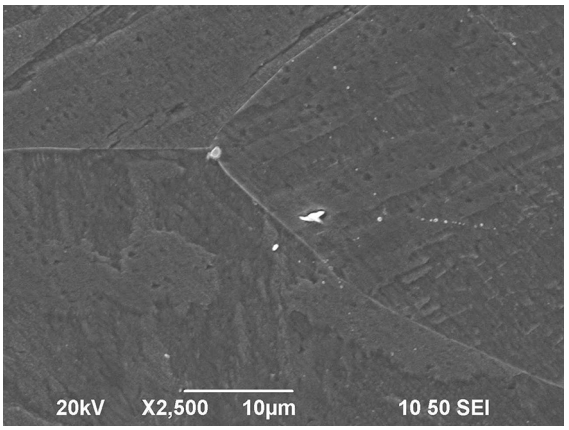

Figure 7. SEM image of solution heat treated specimen. The EDS analysis (Table 4) show that white precipitate is enriched in Mo and Ti (Vilella etch).

4. Discussion

In this study, the effects of aging temperatures, H950 and H1000, on mechanical and corrosion properties of UNS S46500 steel were investigated. The mechanical tests results showed that the tensile strength and elongation of the material is strongly depend to heat treatment applied.

The Thermo-Calc simulation indicated that higher aging temperature produced higher quantity of austenite phase: it was found 0.8% for H950 and 2.9% for H1000 (Table 5). This result is in accordance with Schnitzer et al.[3,20] and Nakagawa and Miyazaki[21] studies.

Austenite acts reducing the tensile strength and increasing the elongation of the material.

The chi phase precipitation was observed for both aging treatments applied for UNS S46500, and the Thermo-Calc analysis indicated that its presence is slight lower for H1000 condition (2.3% for H950 and 1.7% for H1000), in accordance to the observations of this study (Figure 6). The chi phase appeared in the form of relatively coarse precipitates in intergranular and transgranular grain boundaries. Thus,

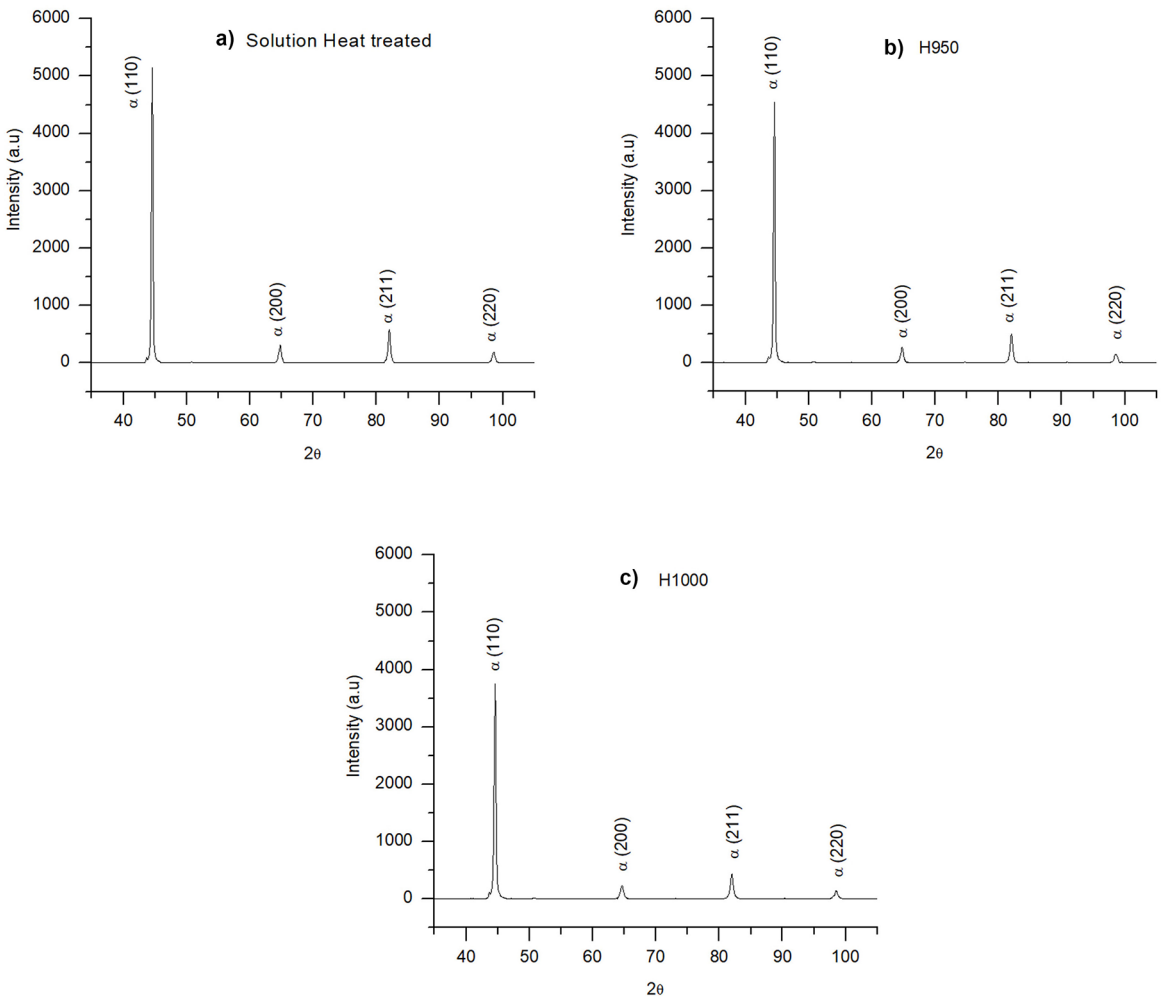

Figure 8. X-ray diffraction patterns of specimens: (a) solution heat treated; (b) H950 and (c) H1000.

the reduction of 2.3% to 1.7% of this phase can contribute to tensile properties reduction. Here the evidence of chi phase is only reported based on termodinamic simulations, nevertheless it was found in literature a research with low carbon martensitic stainless steel and similar Cr and Mo content reporting the presence of Cr and Mo rich precipitates by TEM[22]. This is an evidence that chi phase can appear in this kind of material when the materil is exposed to aging temperatures.

Another factor evaluted is the presence of fine and well distributed Ni_3Ti precipitates in the martensite matrix. As these intermetallic precipitates interact with dislocations, they are the main strengthening mechanism in precipitation hardening steels. Schnitzer et al.[20], in their study for PH 13-8Mo, with nickel aluminum precipitates, calculated that 40% of the loss in yield strength during aging can be attributed to the influence of higher amounts of reverted austenite and the rest of the observed descreased in strength is due to coarsening nickel aluminum precipitates. In fact, the Thermo-Calc (Table 5) results showed that amount of Ni_3Ti precipitates for UNS S46500 did not change significantly with aging temperature (7.2% for H950 and 7.1% for H1000). However, considering that the aging time is identical for the two heat-treatment conditions, in the H1000 condition there is higher temperature for coarsening of precipitates; coarsened Ni_3Ti precipitates and higher austenite content can be the reasons for the lower mechanical resistance of the H1000 condition.

Thus, the results indicated that mechanical properties of H950 and H1000 aging conditions can be atributted to higher

Table 4. Chemical composition of matrix and precipitate of Figure 7.

Elements (wt.%)	Cr	Ni	Ti	Mo	Fe
Matrix	11.81	11.85	2.12	-	74.11
Precipitate	10.63	4.67	16.13	20.85	47.74

Table 5. Phases determined by Thermo-Calc (TCFE8 database).

Phases	510ºC, H950 condition (% vol.)	538ºC, H1000 condition (% vol.)
BCC	86.2	84.3
Ni_3Ti	7.2	7.1
CHI	2.3	1.7
FCC	4.3	6.9

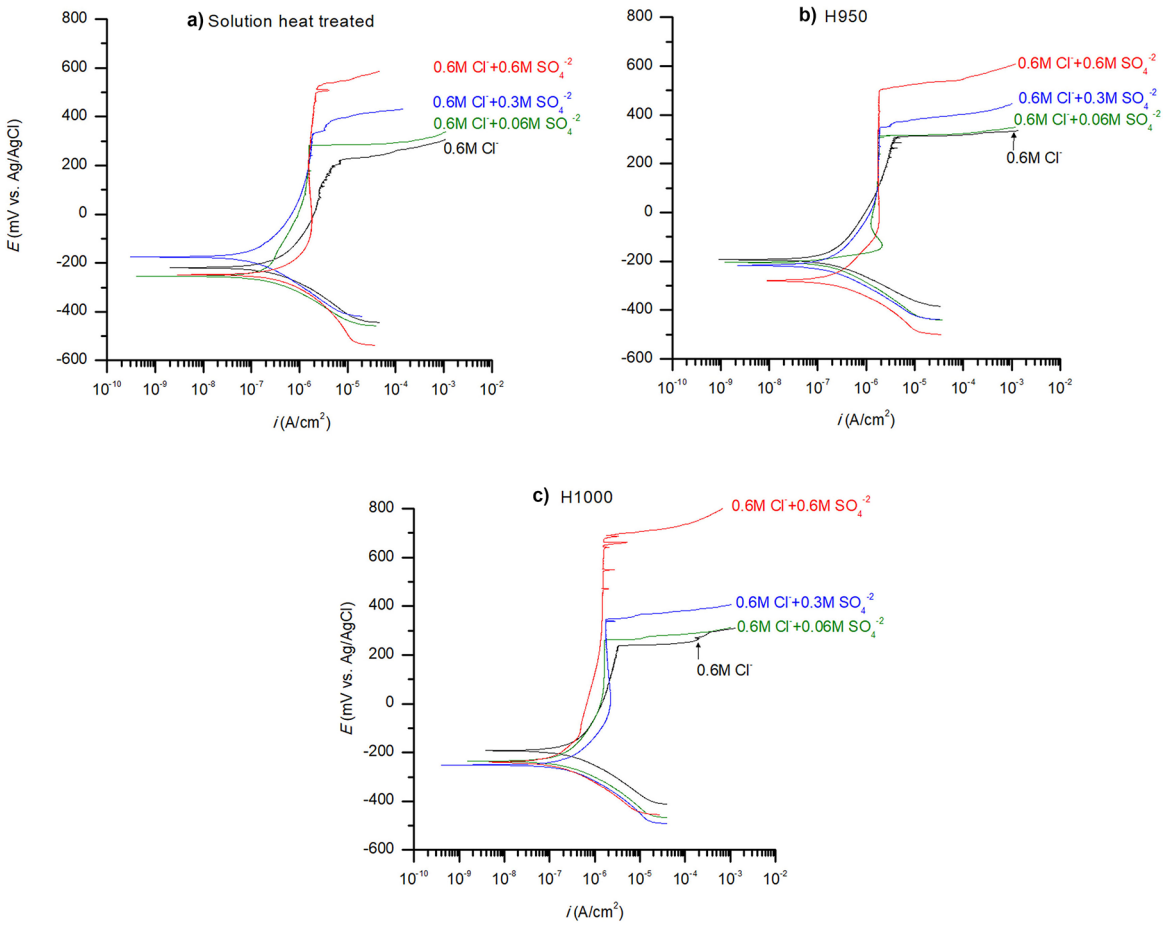

Figure 9. Potentiodynamic polarization curves of UNS S46500 steel on conditions: (a) solution heat treated; (b) H950 and (c) H1000; with increased sulfate additions.

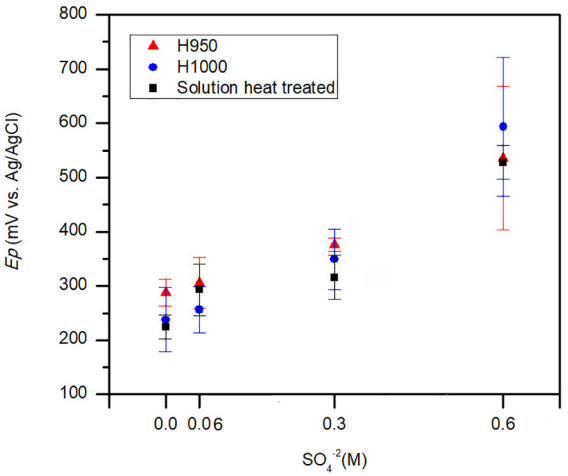

Figure 10. Average pitting potential (Epit) of UNS S46500 in 6M NaCl with sulfate additions.

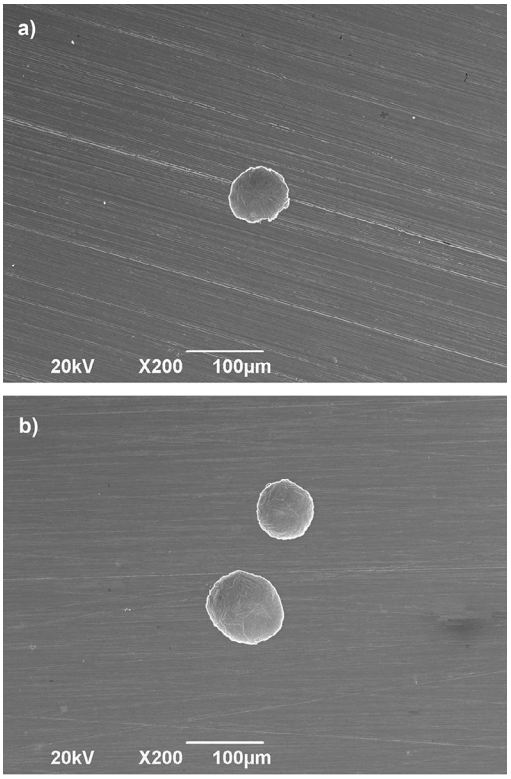

Figure 11. SEM images of pit morphology found at potentiodynamic polarization, conditions: (a) H950 and (b) H1000, 0.6M NaCl + 0.06M Na2SO4 electrolyte.

amount of austenite, diminuish of chi phase and coarsening of Ni_3Ti precipitates.

On the other hand, to evaluate the effect of aging temperature on corrosion resistance, studies[23-24] suggest that material with higher amount of chi phase, as the H950 condition, has a lower resistance to pitting corrosion, since smaller amounts of chromium and molybdenum would be in solid solution. However, the pitting corrosion resistance was very close for all heat treatment conditions studied: solution heat treated, H950 and H1000. Only the sulfate inhibitory effect was more pronounced for the material in the H1000 condition. The mechanism of inhibition of pit nucleation depends upon adsorption of the sulfate ion in the active sites that would initially be occupied by chloride ion, leading to formation of pits. Whereas the chi phase precipitation consumes chromium and molybdenum, leaving the matrix enriched with other elements, particularly nickel, the H1000 condition differs of H950 by having a matrix richer in this element. Seeking in the literature[25], the values of free energy of formation (ΔG^o) for $NiCl_2$ e $NiSO_4$ compounds are -259.4 and -760.9 kJ. mol^{-1}, respectively, which show the chemical affinity between these species. The higher thermodynamic potential for the formation of nickel sulfate compared to the nickel chloride suggests that the adsorption of sulfate is more severe as higher nickel contents are found in solid solution. In this case, this is the condition of the aging heat treatment H1000, resulting in a greater inhibitory effect sulfate for this condition. Is possible to think in the enrichment and depletion of other elements such as Fe, Cr, Mo and Ti. However, thermodynamic data are not found to allow comparison of affinity of these elements with Cl^- and SO_4^{-2}, which is probably owes his lack of chemical affinity.

Another factor that may have contribute to the higher Epit provided with $1Cl^-$: $1SO_4^{-2}$ for H1000 may be related to the amount of interface area that act as adsorption sites. The condition H1000 has higher aging temperature, which has as a consequence higher recovery of dislocations in a martensitic structure, coarsened Ni_3Ti phase and smaller fraction of chi phase. These microstructural changes ultimately reduce the number of interfaces in the microstructure, resulting in smaller amount of adsorption sites.

5. Conclusions

The lower aging temperature (H950 condition) studied in UNS S46500 steel presented greater tensile and yield strengths and hardness due to the presence of minor amounts of austenite, and greater amount of chi phase and Ni_3Ti precipitates finely and uniform distributed throughout the martensite matrix. The two aging conditions, H950 and H1000, have the same pitting corrosion resistance, and the UNS S46500 has excellent response to pitting nucleation inhibition with increasing additions of sulfate.

6. Acknowledgments

The authors would like to acknowledge CNPq (Conselho Nacional de Desenvolvimento Científico e Tecnológico) and CAPES (Coordenação de Aperfeiçoamento de Pessoal de Nível Superior) for their support to the present investigation.

7. References

1. Wert DE, DiSabella RP. *CarTech Custom 465: Advanced Stainless Offers High Strength, Toughness and Corrosion Resistance Wherever Needed*. Wyomissing: Carpenter Technology Corp.; 2006.

2. Wright J, Jung JW, inventors; QuesTek Innovations LLC, assignee. *Martensitic stainless steel strengthened by Ni3Tiη-phase precipitation*. United States patent US7879159B2. 2011 Feb 1.

3. Schnitzer R, Radis R, Nöhrer M, Schober M, Hochfellner R, Zinner S, et al. Reverted austenite in PH13-8 Mo maraging steels. *Materials Chemistry and Physics*. 2010;122(1):138-145.

4. Ravitej SV, Murthy M, Krishnappa MB. Review paper on optimization of process parameters in turning Custom 465(r) precipitation hardened stainless steel. *Materials Today: Proceedings*. 2018;5(1 Pt 3):2787-2794.

5. Daymond BT, Binot N, Schmidt ML, Preston S, Collins R, Shepherd A. Development of Custom 465(r) Corrosion-Resisting Steel for Landing Gear Applications. *Journal of Materials Engineering and Performance*. 2016;25(4):1539-1553.

6. Beraldo CH. *Efeito da temperatura de envelhecimento sobre as propriedades mecânicas e resistência à corrosão por pite do aço inoxidável martensítico endurecido por precipitação UNS S46500*. [Dissertation]. São Paulo: Polytechnic School of University of São Paulo; 2013.

7. Calderón-Hernández JW, Hincapie-Ladino D, de Farias-Azevedo CR, Falleiros NA. Effect of solution heat treatment on the pitting corrosion behavior of a high Mn austenitic stainless steel in chloride solution. *REM: Revista Escola de Minas*. 2015;68(1):91-96.

8. SAE Internacional. *AMS5963 - Steel, Corrosion Resistant, Bars, Wire, and Forgings 12Cr – 11Ni – 1.7Ti – 1Mo Vacuum Induction Plus Vacuum Consumable Electrode Remelted Solution Heat Treated, Precipitation Hardenable*. Warrendale: SAE International; 2007.

9. ASTM International. *ASTM E8/E8M-11 - Standard Test Method for Tension of Metallic Materials*. West Conshohocken: ASTM International; 2011.

10. ASTM International. *ASTM A370-12 - Standard Test Method and Definitions for Mechanical Testing of Steel Products*. West Conshohocken: ASTM International; 2012.

11. Vander Voort GF, ed. *AMS Handbook Volume 09: Metallography and Microstructure*. 9th ed. Materials Park: ASM International; 1985. p. 285-286.

12. Xiang S, Wang JP, Sun YL, Yan YY, Huang SG. Effect of Aging Process on Mechanical Properties of Martensite Precipitation-hardening Stainless Steel. *Advanced Materials Research*. 2011;146-147:382-385.

13. Narendra Babu P, Satyanarayana MVNV, Reddy MGS. Effect of Aging on Mechanical Properties of S465 Stainless Steel. *International Journal for Research in Applied Science & Engineering Technology (IJRASET)*. 2016;4(1):301-306.

14. Lee EU, Goswami R, Jones M, Vasudevan AK. Environment-Assisted Cracking in Custom 465 Stainless Steel. *Metallurgical and Materials Transactions A*. 2011;42(2):415-423.

15. Ifergane S, Pinkas M, Barkay Z, Brosh E, Ezersky V, Beeri O, et al. The relation between aging temperature, microstructure evolution and hardening of Custom 465(r) stainless steel. *Materials Characterization*. 2017;127:129-136.

16. Bechtoldt CJ, Vacher HC. Phase-Diagram Study of Alloys in the Iron-Chromium-Molybdenum-Nickel System. *Journal of Research of National Bureau of Standards*. 1957;58(1):7-19.

17. Leckie HP, Uhlig HH. Environmental Factors Affecting the Critical Potential for Pitting in 18-8 Stainless Steel. *Journal of the Electrochemical Society*. 1966;113(12):1262-1267.

18. Sato N, Kudo K, Noda T. The anodic oxide film on iron in neutral solution. Electrochimica Acta. 1971;16(11):1909-1921.

19. Calderón Hernández JW. *Efeito da temperatura de solubilização e da concentração de íons cloreto e sulfato sobre a resistência à corrosão por Pite dos aços inoxidáveis austeníticos 17Cr-6Mn-5Ni e UNS S30403*. [Dissertation]. São Paulo: Polytechnic School of University of São Paulo; 2012.

20. Schnitzer R, Zickler GA, Lach E, Clemens H, Zinner S, Lippmann T, et al. Influence of reverted austenite on static and dynamic mechanical properties of a PH 13-8 Mo maraging steel. *Material Science and Engineering: A*. 2010;527(7-8):2065-2070.

21. Nakagawa H, Miyazaki T. Effect of retained austenite on the microstructure and mechanical properties of martensitic precipitation hardening stainless steel. *Journal of Material Science*. 1999;34(16):3901-3908.

22. Ma X, Wang L, Subramanian SV, Liu C. Studies on Nb Microalloying of 13Cr Super Martensitic Stainless Steel. *Metallurgical and Materials Transactions A*. 2012;43(12):4475-4486.

23. Wegrelius L, Olefjord I. Dissolution and Passivation of Stainless Steels Eposed to Hydrochloric Acid. *Materials Science Forum*. 1995;185-188:347-356.

24. Calderón-Hernández JW, Hincapie-Ladino D, Martins Filho EB, Magnabosco R, Alonso-Falleiros N. Relation Between Pitting Potential, Degree of Sensitization, and Reversed Austenite in a Supermartensitic Stainless Steel. *Corrosion*. 2017;73(8):953-960.

25. Weast RC. *Handbook of Chemistry and Physics*. 1st Student ed. Boca Raton: CRC Press; 1988.